

Comparing the Weighted Density Approximation with the LDA and GGA for Ground State Properties of Ferroelectric Perovskites

Zhigang Wu and R.E. Cohen

*Geophysical Laboratory, Carnegie Institution of Washington,
5251 Broad Branch Road, NW, Washington, DC 20015*

D.J. Singh

*Center for Computational Materials Science,
Naval Research Laboratory, Washington, DC 20375*

(Dated: October 24, 2018)

Abstract

First-principles calculations within the weighted density approximation (WDA) were performed for ground state properties of ferroelectric perovskites PbTiO_3 , BaTiO_3 , SrTiO_3 , KNbO_3 and KTaO_3 . We used the plane-wave pseudopotential method, a pair distribution function G based on the uniform electron gas, and shell partitioning. Comparing with the local density approximation (LDA) and the general gradient approximation (GGA), we found that the WDA significantly improves the equilibrium volume of these materials in cubic symmetry over both the LDA and GGA; Ferroelectric instabilities calculated by the WDA agree with the LDA and GGA very well; At the experimental ferroelectric lattice, optimized atom positions by the WDA are in good agreement with measured data; However the WDA overestimates the strain of tetragonal PbTiO_3 at experimental volume; The WDA overestimates the volume of fully relaxed structures, but the GGA results are even worse. Some calculations were also done with other models for G . It is found that a G with longer range behavior yields improved relaxed structures. Possible avenues for improving the WDA are discussed.

I. INTRODUCTION

Since the early 1980s, first-principles calculations based on the density functional theory (DFT) have been implemented to compute diverse properties of piezoelectric and ferroelectric materials. The main difficulty within the DFT is how to treat the exchange-correlation (xc) energy accurately, because the exact form of it remains unknown. The local density approximation (LDA), in which the xc energy density (ϵ_{xc}) depends only on local charge density, dominated these calculations due to its simplicity and surprising success. When performed at the experimental volume, the LDA predicts many properties of ferroelectric materials, such as phonon frequencies, ferroelectric phase transitions, polarization, elasticity, etc., with extraordinary accuracy [1]. However it is well known that the LDA overestimates the binding energy, and underestimates the bond length by 1-2%, which results in the calculated equilibrium volume normally 3-6% less than experiment. On the other hand, ferroelectric properties are extremely sensitive to volume. For example, the ferroelectric instabilities in BaTiO₃ [2] and KNbO₃ [3, 4, 5, 6] are severely reduced, if not totally eliminated, at the LDA zero pressure volume. Even at the experimental volume, the LDA incorrectly predict certain properties, e.g., it overestimates the strain of the tetragonal PbTiO₃ [1] and the static dielectric constant ϵ_∞ [7, 8], and it underestimates the band gap [9, 10].

The generalized gradient approximation (GGA) [11, 12], which includes the density gradients, is the natural next step beyond the LDA. Generally speaking, the semi-local GGA tends to improve upon the LDA in many aspects, especially for atomic energies and structural energy differences [12, 13, 14]. For ferroelectric properties and band gaps, the GGA normally predicts very similar results to the LDA at experimental volume. However the GGA tends to overestimate the bond length by about 1% [6, 15]. To illustrate this we present a full relaxation of tetragonal $P4mm$ PbTiO₃ within both the LDA (Hedin-Lundqvist [16]) and the GGA (The PBE [12] version was used throughout this paper.) using the linearized augmented planewave method with local orbital extensions (LAPW+LO) [17]. As seen in Table I, at the experimental volume, the GGA predicts a strain better than the LDA, but the fully relaxed GGA structure is much worse than that of the LDA. We also used the ABINIT package [18, 19], which is based on pseudopotentials and a planewave basis. For the fully relaxed tetragonal PbTiO₃, the LDA predicts a volume of 60.34 Å³, and $c/a = 1.042$, while the GGA gives a volume of 70.54 Å³, and $c/a = 1.24$. The ABINIT results are in excellent

agreement with the LAPW results. The failures of the LDA and GGA indicate that more complicated non-local approximations are needed.

The weighted density approximation (WDA) [20, 21, 22], within which ϵ_{xc} depends on charge density over a finite region, was advanced in the late 1970's. The WDA assumes that any inhomogeneous electron gas can be regarded as continuously being deformed from a homogeneous electron gas, so the real pair-distribution function of the inhomogeneous gas can be replaced by that of a homogeneous gas at every point with certain weighted density. By constructing a model xc hole, the sum rule is fulfilled. One problem that both the LDA and the GGA have is the self-interaction error, i.e., the imperfect cancellation of Hartree and xc terms in the one-electron limit. The self-interaction-correction (SIC) method [23] predicts band gaps of transition-metal oxides in good agreement with experiments [24]. It demonstrates the importance of SIC. However the SIC method is not efficient because its potential is orbital-dependent. The WDA is free of self-interaction for the one-electron limit, and its potential is directly a functional of the charge density, and not orbital dependent. For the non-local (uniform) limit, it reduces to the LDA. It has been reported that the WDA significantly improves atomic energies [22, 25] and the equilibrium volume of some simple bulk solids [26] over the LDA. It is promising to apply the WDA for ground state properties of more complicated ferroelectric perovskites.

The selected perovskites PbTiO_3 , BaTiO_3 , SrTiO_3 , KNbO_3 and KTaO_3 are both technically and theoretically important ferroelectric materials. They are also prototypes of more complicated and interesting ferroelectric relaxors such as $(1-x)\text{Pb}(\text{Mg}_{1/3}\text{Nb}_{2/3})\text{O}_3-x\text{PbTiO}_3$ (PMN-PT) and $(1-x)\text{Pb}(\text{Zn}_{1/3}\text{Nb}_{2/3})\text{O}_3-x\text{PbTiO}_3$ (PZN-PT). They have previously been studied extensively to understand ferroelectricity [2, 3, 4, 5, 6, 27, 28]. In this paper, first a brief overview of the WDA formalism will be presented in section II. Then we will report the WDA results of ground state properties of these perovskites in section III. In section IV, we discuss avenues for improving the WDA focussing on the symmetry under particle exchange in the pair correlation function.

II. FORMALISM

The general form of the xc energy in the DFT scheme can be expressed as (All equations are in atomic units, $\hbar = m = e^2 = 1$.)

$$E_{\text{xc}}[n] = \frac{1}{2} \int n(\mathbf{r}) d\mathbf{r} \int \frac{\bar{n}_{\text{xc}}(\mathbf{r}, \mathbf{r}')}{|\mathbf{r} - \mathbf{r}'|} d\mathbf{r}', \quad (1)$$

here the xc hole density $\bar{n}_{\text{xc}}(\mathbf{r}, \mathbf{r}')$ is defined as

$$\begin{aligned} \bar{n}_{\text{xc}}(\mathbf{r}, \mathbf{r}') &= n(\mathbf{r}') \int_0^1 [\bar{g}_{\text{xc}}^n(\mathbf{r}, \mathbf{r}'; \lambda) - 1] d\lambda \\ &\equiv n(\mathbf{r}') [\bar{g}_{\text{xc}}^n(\mathbf{r}, \mathbf{r}') - 1], \end{aligned} \quad (2)$$

where $\bar{g}_{\text{xc}}^n(\mathbf{r}, \mathbf{r}')$ is the coupling-constant averaged pair-distribution function of a system with a density $n(\mathbf{r})$ [29]. This function is symmetric

$$\bar{g}_{\text{xc}}^n(\mathbf{r}, \mathbf{r}') = \bar{g}_{\text{xc}}^n(\mathbf{r}', \mathbf{r}), \quad (3)$$

and the xc hole satisfies the following sum rule

$$\int \bar{n}_{\text{xc}}(\mathbf{r}, \mathbf{r}') d\mathbf{r}' = -1. \quad (4)$$

Although the function \bar{g}_{xc} of a uniform gas is known with high accuracy based on Monte Carlo simulations [30], the exact form of $\bar{g}_{\text{xc}}^n(\mathbf{r}, \mathbf{r}')$ is still elusive for an arbitrary inhomogeneous system. Different density approximations make different approximations to \bar{g}_{xc} . In the WDA approach $\bar{g}_{\text{xc}}^n(\mathbf{r}, \mathbf{r}')$ is approximated by a model function G (e.g., a uniform type),

$$G[|\mathbf{r} - \mathbf{r}'|, \bar{n}(\mathbf{r})] = \bar{g}_{\text{xc}}^n(\mathbf{r}, \mathbf{r}') - 1, \quad (5)$$

where the parameter $\bar{n}(\mathbf{r})$ is the weighted density, and it can be determined from the sum rule

$$\int n(\mathbf{r}') G[|\mathbf{r} - \mathbf{r}'|, \bar{n}(\mathbf{r})] d\mathbf{r}' = -1. \quad (6)$$

By definition, the function G is not symmetric

$$G(\mathbf{r}, \mathbf{r}') \neq G(\mathbf{r}', \mathbf{r}). \quad (7)$$

Since $\bar{n}(\mathbf{r})$ is only a function of \mathbf{r} , not \mathbf{r}' , it leads to wrong asymptotic behavior at the low density limit [22], which we will discuss in section IV.

The natural choice of G would be obtained from g for a uniform electron gas, but since the systems of interest are inhomogeneous, other types of model function G could be better [31, 32]. Among them, the Gunnarsson-Jones (GJ [31]) ansatz ensures the correct behavior at large distance

$$G^{\text{GJ}}(r, n) = c_1(n) \left\{ 1 - \exp\left(-\left[\frac{r}{c_2(n)}\right]^{-5}\right) \right\}, \quad (8)$$

while Rushton *et al.* (RTZ [33]) used a simple Gaussian function

$$G^{\text{RTZ}}(r, n) = c_1(n) \exp\left(-\left[\frac{r}{c_2(n)}\right]^2\right), \quad (9)$$

which resembles the exact one for the short distance limit, and it is also a good approximation to the uniform G . The parameters c_1 and c_2 can be determined from the following conditions

$$n \int G(r, n) d^3r = -1, \quad (10)$$

$$n \int \frac{G(r, n)}{r} d^3r = \epsilon_{\text{xc}}^{\text{hom}}(n), \quad (11)$$

where $\epsilon_{\text{xc}}^{\text{hom}}(n)$ is the xc energy density of a homogeneous gas with density n .

The WDA xc energy is

$$E_{\text{xc}}^{\text{WDA}}[n] = \frac{1}{2} \int \int \frac{n(\mathbf{r})n(\mathbf{r}')}{|\mathbf{r} - \mathbf{r}'|} G[|\mathbf{r} - \mathbf{r}'|, \bar{n}(\mathbf{r})] d\mathbf{r} d\mathbf{r}', \quad (12)$$

and the corresponding xc potential $v_{\text{xc}}(\mathbf{r})$ is the functional derivative of E_{xc} ,

$$v_{\text{xc}}^{\text{WDA}}(\mathbf{r}) = \frac{\delta E_{\text{xc}}^{\text{WDA}}[n]}{\delta n(\mathbf{r})} = v_1(\mathbf{r}) + v_2(\mathbf{r}) + v_3(\mathbf{r}), \quad (13)$$

where

$$v_1(\mathbf{r}) = \frac{1}{2} \int \frac{n(\mathbf{r}')}{|\mathbf{r} - \mathbf{r}'|} G[|\mathbf{r} - \mathbf{r}'|, \bar{n}(\mathbf{r})] d\mathbf{r}' = \epsilon_{\text{xc}}^{\text{WDA}}(\mathbf{r}), \quad (14)$$

$$v_2(\mathbf{r}) = \frac{1}{2} \int \frac{n(\mathbf{r}')}{|\mathbf{r} - \mathbf{r}'|} G[|\mathbf{r} - \mathbf{r}'|, \bar{n}(\mathbf{r}')] d\mathbf{r}', \quad (15)$$

$$v_3(\mathbf{r}) = \frac{1}{2} \int \int \frac{n(\mathbf{r}')n(\mathbf{r}'')}{|\mathbf{r}' - \mathbf{r}''|} \frac{\delta G[|\mathbf{r}' - \mathbf{r}''|, \bar{n}(\mathbf{r}')]}{\delta n(\mathbf{r})} d\mathbf{r}' d\mathbf{r}'' . \quad (16)$$

Examination of the above suggests that implementation of $E_{\text{xc}}^{\text{WDA}}$ and $v_{\text{xc}}^{\text{WDA}}(\mathbf{r})$ could be cumbersome. However, in a plane-wave representation, by using the convolution theorem, these terms can be evaluated efficiently, as detailed in Ref. [26].

One subtle issue in the WDA implementation is shell partitioning [22]. The WDA scheme does not describe the exchange interaction between core and valence states very well because

of the use of local $\bar{n}(\mathbf{r})$ in the model function G . Physically the range of integration of G is similar to the size of atoms, and there is no distinction between core and valence electrons to the contribution of E_{xc}^{WDA} . As a result core and valence electrons dynamically screen valence electrons equally, which leads to non-zero exchange energy between core and valence states outside core regions. On the other hand, the LDA can give correct inter-shell contributions, since the LDA depends only on local density, and the core density vanishes outside core regions. Based on this observation, a shell partitioning approach was proposed [22, 26], in which the valence-valence interactions are treated with the WDA, while core-core and core-valence interactions with the LDA. The total xc energy is written

$$E_{xc}[n] = E_{xc}^{\text{LDA}}[n] + E_{xc}^{\text{WDA}}[n_v] - E_{xc}^{\text{LDA}}[n_v], \quad (17)$$

where n_v is the valence density and n is the total density. The sum rule becomes

$$\int \{n_v(\mathbf{r}')G[|\mathbf{r} - \mathbf{r}'|, \bar{n}(\mathbf{r})] + n_c(\mathbf{r})G[|\mathbf{r} - \mathbf{r}'|, n(\mathbf{r})]\} d\mathbf{r}' = -1, \quad (18)$$

where n_c is the core density. Ref [34] shows why this sum rule must be used instead of a simpler one $\int \{n_v(\mathbf{r}')G[|\mathbf{r} - \mathbf{r}'|, \bar{n}(\mathbf{r})] = -1$. The corresponding v_{xc} for core and valence states will be different since E_{xc} depends explicitly on both core and valence density. The detailed derivation and formulas can be found in the appendix of Ref. [35]. We can still use the Hellmann-Feynmann theorem [36] to determine atomic forces, and we found that the directly calculated forces agree with the numerical results of finite energy difference very well with the WDA shell partitioning.

III. RESULTS

A. Technical details

The WDA was implemented [26] within a plane-wave basis pseudopotential method. The pseudopotentials are of the hard Troullier-Martins type [37]. The semi-core states of metal ions include $3s$ and $3p$ states of K and Ti, $4s$ and $4p$ states of Nb and Sr, $5s$ and $5p$ states of Ta and Ba, and $5d$ states of Pb. $2s$ states of O are also treated as semi-core. We used the WDA for valence states, the LDA for semi-core states, and pseudized lower states. Plane-wave basis sets with cut-off of 132 Ry were tested and found to be highly converged. A $4 \times 4 \times 4$ \mathbf{k} -point mesh was exploited except for frozen-phonon soft-mode calculations of

rhombohedral BaTiO₃ and KNbO₃, where a denser $6 \times 6 \times 6$ \mathbf{k} -mesh was used because the ferroelectric double well depth is only about 2-3 mRy. The standard 3-point interpolation was employed to obtain $\bar{n}(\mathbf{r})$ with a logarithmic grid of increment $\bar{n}_{i+1} = 1.25\bar{n}_i$. We tested the convergence by the 6-point interpolation which makes negligible difference. For the function G , we used a uniform type [38] for the following calculations. In the last part of this section we will also present results with other types of G .

B. Equilibrium volume of cubic structures

We first calculated the lattice constant of these materials constrained in cubic symmetry. The experimental values in Table II are those extrapolated to $T = 0$. The zero point corrections are expected to be less than 0.3%. As mentioned before, the LDA lattice constant is about 1-2% less than experiment, and this small error is big enough to make many ferroelectric properties incorrect. On the other hand, the GGA results are better than the LDA, but they are a little too large for BaTiO₃, SrTiO₃, and KTaO₃. The WDA dramatically improves the lattice constant over the LDA, and it is also better than the GGA. Actually all these WDA lattice constants are very close to experimental data except for PbTiO₃. At low temperature PbTiO₃ is tetragonal with a big strain of 6%, and other four perovskites are very close to the cubic structure. The extrapolation of the high temperature cubic data of PbTiO₃ therefore is not expected to be as reasonable as the other cases.

C. Ferroelectric instabilities

We studied the ferroelectric instability in tetragonal PbTiO₃ and rhombohedral BaTiO₃ and KNbO₃. We displaced atom positions according to the experimental soft-mode distortion patterns at the experimental lattice. For tetragonal PbTiO₃ $c/a = 1.063$, while for rhombohedral BaTiO₃ and KNbO₃, we neglected the tiny lattice distortion from the cubic structure. As mentioned before, the LDA and GGA describes the ferroelectric instability very well at the experimental structure, so one may hope that the WDA retains this good feature. Fig. 1 shows the calculated curves of energy versus ferroelectric displacement along [001] for PbTiO₃ and [111] for BaTiO₃ and KNbO₃. In all cases, the WDA curves match with the LDA ones very well. It shows that the WDA can predict ferroelectric phase transi-

tions as well as the LDA. On the other hand, the GGA predicts a smaller energy difference between paraelectric and ferroelectric states of PbTiO_3 than the LDA, but agrees well with the LDA for BaTiO_3 and KNbO_3 .

D. Structural optimization

Since there is no difficulty calculating atomic forces with the WDA approach, we performed structural optimization for tetragonal $P4mm$ PbTiO_3 and rhombohedral $P3m1$ BaTiO_3 and KNbO_3 . First we only optimized internal parameters at experimental lattices, and the relaxed atomic positions are shown in Tables III, IV and V for PbTiO_3 , BaTiO_3 and KNbO_3 respectively. In all cases, the LDA, GGA, and WDA predict very similar results which are in good agreement with experiment except for KNbO_3 whose theoretical displacements from ideal positions are about 30% less than measured data [39]. The consistency of theoretical results suggests re-examination of these experimental data.

We also did full relaxations for the above materials. At the experimental volume, the WDA predicts $c/a = 1.106$ for PbTiO_3 , which is close to the LDA value of 1.112, while the GGA gives $c/a = 1.068$. Compared with the measured value of 1.063, the WDA is not as good as the GGA in this case. For the fully relaxed structure, the WDA predicts a large $c/a = 1.19$ and a volume 8.2% bigger than experiment, which are poorer than the LDA, but still a little better than the GGA. To demonstrate that this is not because of poor pseudopotentials or other problems in the planewave method, we compared the energy difference between the LDA equilibrium structure and the WDA equilibrium structure. For the LDA, the planewave code predicts -11.8 mRy, while the LAPW gives -12.3 mRy. It proves that the planewave method is reliable. On the other hand, the WDA energy difference is 9.4 mRy, which is similar in magnitude with opposite sign. We also calculated the equilibrium structures of rhombohedral BaTiO_3 and KNbO_3 , as shown in Table VI. We can conclude that the LDA underestimates the fully relaxed volume by almost the same amount as constrained in the cubic structure, while the WDA overestimates it, and the GGA overestimates it even more.

E. Results with other G functions

Because there is no reason for the uniform G to be the best choice, we also tried other types of function G . We denote the uniform type as (a), the GJ type as (b), the simple Gaussian (RTZ) type as (c), and type (d) as $G(r, n) = c_1(n)\exp(-[\frac{r}{c_2(n)}]^6)$. To clearly visualize them, we show these functions together at $n = 1.0$ in Fig. 2. The simple Gaussian type is a good approximation to the uniform G , the type (d) has longer interaction range than others, and the GJ type agrees with the uniform one when $r > 1.745$.

We recalculated the equilibrium lattice constants of the cubic structure with the other three G s. As shown in Table VII, the newly calculated lattice constants are very similar. Compared with the previous (uniform G) results, the GJ type predicts slightly larger lattice constants, while the simple Gaussian form and type (d) predict slightly smaller ones.

However the choice of G is more sensitive for the fully relaxed structure. Comparing with the uniform G , We found that the GJ type predicts even worse results, the simple Gaussian gives very similar results, and the type (d) is particularly better. For tetragonal PbTiO_3 at experimental volume, its optimized c/a becomes 1.078, and for the fully relaxed structure c/a is 1.092 and the volume is only 0.8% larger than experiment. However, as listed in Table VIII, the volumes of rhombohedral BaTiO_3 and KNbO_3 do not improve as much as that of tetragonal PbTiO_3 , they are still 2.4% and 1.3% larger than experiment respectively.

We could further improve the WDA results by tuning the shape of function G , but it is hard to justify, and also it is difficult to make a single G to fit all properties of all materials. We need a simple and reasonable G , such as the uniform one, which can predict good ground state properties for both the cubic and the fully relaxed structures. Actually since different G s predict very similar equilibrium volumes for the cubic structure, we expect their results for the fully relaxed structure should also be similar to the cubic structure, just like the LDA. So we focus on the WDA method itself. If one draws energy versus volume curves for the cubic and optimized tetragonal PbTiO_3 as shown in Fig. 3, one can see that the WDA curves for the cubic structure have similar curvatures to the LDA one, while for the tetragonal structure the WDA curves are too flat on the right side in comparison with the LDA. It means that for the relaxed structure the WDA predicts an energy increase smaller than expected on the large volume side. This suggests an asymptotic problem, as is discussed in the next section.

IV. DISCUSSIONS AND PROSPECTS

A. Asymptotic behavior

An accurate functional approximation should fulfill at least some of the following conditions: (1) sum rule of the xc hole; (2) for a slowly varying density, it should recover the uniform gas limit; (3) absence of self-interaction; (4) asymptotic properties of xc energy and potential. One may verify that from the exact DFT expression (Eq. 1) the xc energy density $\epsilon_{xc}(\mathbf{r})$ far away from the nucleus (low density limit) are

$$\lim_{r \rightarrow \infty} \epsilon_{xc}(\mathbf{r}) \rightarrow -\frac{1}{2r}. \quad (19)$$

Since $g_{xc}^n(\mathbf{r}, \mathbf{r}')$ is symmetric, one can derive that

$$v_{xc}(\mathbf{r}) = 2\epsilon_{xc}(\mathbf{r}) + v_3(\mathbf{r}), \quad (20)$$

and because $\frac{\delta g_{xc}^n(\mathbf{r}', \mathbf{r}'')}{\delta n(\mathbf{r})}$ vanishes exponentially in the above limit,

$$\lim_{r \rightarrow \infty} v_{xc}(\mathbf{r}) \rightarrow -\frac{1}{r}. \quad (21)$$

The asymptotic conditions 19 and 21 are the consequence of requirement of cancellation of self-interaction in the Hartree terms. They look simple, but are very difficult to fulfill simultaneously. One can easily construct an energy or a potential satisfying the above conditions separately, but difficulty arises in making $v_{xc}(\mathbf{r})$ as the functional derivative of $E_{xc}[n(\mathbf{r})]$. In the LDA and GGA, both $\epsilon_{xc}(\mathbf{r})$ and $v_{xc}(\mathbf{r})$ go to zero exponentially for large r . Asymptotically they are less attractive than they should be. In the WDA, $\epsilon_{xc}^{\text{WDA}}(\mathbf{r})$ satisfies condition 19, but the unsymmetrical function G (Eq. 7) leads to $v_1(\mathbf{r}) \neq v_2(\mathbf{r})$, and $v_2(\mathbf{r})$ goes to zero exponentially also, giving that $v_{xc}^{\text{WDA}}(\mathbf{r})$ at large r to be the same as $\epsilon_{xc}^{\text{WDA}}(\mathbf{r})$

$$\lim_{r \rightarrow \infty} v_{xc}^{\text{WDA}}(\mathbf{r}) \rightarrow -\frac{1}{2r}, \quad (22)$$

which is off by a factor of 1/2.

The correct asymptotic behavior of $\epsilon_{xc}^{\text{WDA}}(\mathbf{r})$ is due to the correct handling self-interaction in the WDA, while the wrong asymptotic behavior of $v_{xc}^{\text{WDA}}(\mathbf{r})$ results from the violated symmetry of G under exchange $(\mathbf{r}, \mathbf{r}') \longleftrightarrow (\mathbf{r}', \mathbf{r})$. In order to overcome this problem so that the WDA will behave closer to the exact DFT and eventually it will circumvent its failure for the fully relaxed structure, we can symmetrize G .

B. A new approach: symmetrization of the WDA

A symmetric G satisfying Eq. 3 will make both $\epsilon_{xc}^{\text{WDA}}(\mathbf{r})$ and $v_{xc}^{\text{WDA}}(\mathbf{r})$ have the correct asymptotic behavior. The simplest approach is to make G depends on the weighted density at both \mathbf{r} and \mathbf{r}' , for example, a sum form would be

$$G^{\text{SWDA}}(\mathbf{r}, \mathbf{r}') \equiv \frac{1}{2}\{G[|\mathbf{r} - \mathbf{r}'|, \bar{n}(\mathbf{r})] + G[|\mathbf{r} - \mathbf{r}'|, \bar{n}(\mathbf{r}')]\}, \quad (23)$$

and

$$G^{\text{SWDA}}(\mathbf{r}, \mathbf{r}') = G^{\text{SWDA}}(\mathbf{r}', \mathbf{r}). \quad (24)$$

Now we have $v_1(\mathbf{r}) = v_2(\mathbf{r}) = \epsilon_{xc}(\mathbf{r})$, and the conditions 19 and 21 are fulfilled naturally.

The corresponding sum rule will be

$$\int n(\mathbf{r}')G^{\text{SWDA}}(\mathbf{r}, \mathbf{r}')d\mathbf{r}' = \frac{1}{2} \int n(\mathbf{r}')\{G[|\mathbf{r} - \mathbf{r}'|, \bar{n}(\mathbf{r})] + G[|\mathbf{r} - \mathbf{r}'|, \bar{n}(\mathbf{r}')]\}d\mathbf{r}' = -1. \quad (25)$$

Self-consistent iteration can be used to determine $\bar{n}(\mathbf{r})$. Once $\bar{n}(\mathbf{r})$ is known, E_{xc}^{SWDA} is known also. The difficulty arises when one wants to calculate $v_3(\mathbf{r})$. If it can be determined efficiently, this symmetrized WDA will satisfy all the conditions listed in the beginning of last subsection, so this new WDA is very promising. It would overcome the problems that lead to shell partitioning because core and valence states would be distinguishable to screen valence electrons.

V. CONCLUSIONS

In conclusion, we calculated ground state properties of some common ferroelectric perovskites with the WDA. Compared with results of the LDA and GGA, the WDA describes properties of systems with the cubic symmetry or at experimental ferroelectric lattices very well, but it fails to predict good fully optimized structure. The symmetry problem of function G could cause this failure. A new approach is proposed, and efforts must be taken to circumvent the mathematical difficulty.

VI. ACKNOWLEDGMENTS

This work was supported by the Office of Naval Research under ONR Grants N00014-02-1-0506 and N0001403WX20028. Work at NRL is supported by the Office of Naval Research.

Calculations were done on the Center for Piezoelectrics by Design (CPD) computer facility, and on the Cray SV1 supported by NSF and the Keck Foundation. We are grateful for discussions with H. Krakauer, M. Pederson, I. Mazin, D. Vanderbilt, N. Choudhury, A. Asthagiri, M. Sepliarsky, M. Gupta and R. Gupta. We also thank E. Walter and M. Barnes for helping us to smooth out computations on the CPD cluster.

- [1] See e.g., R.E. Cohen, *J. Phys. Chem. Solids* **61**, 139-146 (1999).
- [2] R.E. Cohen, and H. Krakauer, *Phys. Rev. B* **42**, 6416 (1990); R.E. Cohen, *Nature (London)* **358**, 136 (1992); R.E. Cohen, and H. Krakauer, *Ferroelectrics* **136**, 65 (1992).
- [3] D.J. Singh, and L.L. Boyer, *Ferroelectrics* **136**, 95 (1992).
- [4] A.V. Postnikov, T. Neumann, G. Borstel, and M. Methfessel, *Phys. Rev. B* **48**, 5910 (1993); A.V. Postnikov, T. Neumann, and G. Borstel, *Ferroelectrics* **164**, 101 (1995).
- [5] R. Yu, and H. Krakauer, *Phys. Rev. Lett.* **74**, 4067 (1995); C.-Z. Wang, R. Yu, and H. Krakauer, *Ferroelectrics* **194**, 97 (1997).
- [6] D.J. Singh, *Ferroelectrics* **164**, 143 (1995); *Ferroelectrics* **194**, 299 (1997).
- [7] A. Dal Corso, S. Baroni, and R. Resta, *Phys. Rev. B* **49**, 5323 (1994).
- [8] R. Resta, *Ferroelectrics* **194**, 1 (1997); S. Dallolio, R. Dovesi, and R. Resta, *Phys. Rev. B* **56**, 10105 (1997).
- [9] D.R. Hamann, *Phys. Rev. Lett.* **42**, 662 (1979).
- [10] M.T. Yin, and M.L. Cohen, *Phys. Rev. B* **26**, 5668 (1982).
- [11] D.C. Langreth, and M.J. Mehl, *Phys. Rev. B* **28**, 1809 (1983); A.D. Becke, *Phys. Rev. A* **38**, 3098 (1988).
- [12] J.P. Perdew, K. Burke, and M. Ernzerhof, *Phys. Rev. Lett.* **77**, 3865 (1996).
- [13] J.P. Perdew, J.A. Chevary, S.H. Vosko, K.A. Jackson, M.R. Pederson, D.J. Singh, and C. Fiolhais, *Phys. Rev. B* **46**, 6671 (1992); *Phys. Rev. B* **48**, 4978(E) (1993).
- [14] B. Hammer, K.W. Jacobsen, and J.K. Norskov, *Phys. Rev. Lett.* **70**, 3971 (1993); B. Hammer, and M. Scheffler, *Phys. Rev. Lett.* **74**, 3487 (1995).
- [15] C. Filippi, D.J. Singh, and C.J. Umrigar, *Phys. Rev. B* **50**, 14947 (1994).
- [16] L. Hedin, and B.I. Lundqvist, *I. Phys. C* **4**, 2064 (1971).
- [17] D.J. Singh, *Planewaves, Pseudopotentials and LAPW method* (Kluwer Academic publishers,

- Boston, 1994).
- [18] X. Gonze, J.-M. Beuken, R. Caracas, F. Detraux, M. Fuchs, G.-M. Rignanese, L. Sindic, M. Verstraete, G. Zerah, F. Jollet, M. Torrent, A. Roy, M. Mikami, Ph. Ghosez, J.-Y. Raty, D.C. Allan, *Comput. Mater. Sci.* **25**, 478 (2002).
 - [19] The ABINIT code is a common project of the Universit Catholique de Louvain, Corning Incorporated, and other contributors (URL <http://www.abinit.org>).
 - [20] O. Gunnarsson, M. Jonson, and B.I. Lundquist, *Phys. Lett.* **59A**, 177 (1976); O. Gunnarsson, M. Jonson, and B.I. Lundquist, *Solid State Commun.* **24**, 765 (1977).
 - [21] J.A. Alonso, and L.A. Girifalco, *Phys. Rev. B* **17**, 3735 (1978).
 - [22] O. Gunnarsson, M. Jonson, and B.I. Lundqvist, *Phys. Rev. B* **20**, 3136 (1979).
 - [23] J.P. Perdew and A. Zunger, *Phys. Rev. B* **23**, 5048 (1981).
 - [24] A. Svane, and O. Gunnarsson, *Phys. Rev. Lett.* **65**, 1148 (1990); Z. Szotek, W.M. Temmerman, and H. Winter, *Phys. Rev. B* **47**, 4029 (1993).
 - [25] O.V. Gritsenko, A. Rubio, L.C. Balbás, and J.A. Alonso, *Chem. Phys. Lett.* **205**, 348 (1993).
 - [26] D.J. Singh, *Phys. Rev. B* **48**, 14099 (1993).
 - [27] D.J. Singh, *Phys. Rev. B* **53**, 176 (1996).
 - [28] C. Lasota, C. Wang, R. Yu, and H. Krakauer, *Ferroelectrics* **194** 109 (1997).
 - [29] O. Gunnarsson, and B.I. Lundqvist, *Phys. Rev. B* **13**, 4274 (1976).
 - [30] J.P. Perdew, and Yue Wang, *Phys. Rev. B* **46**, 12947 (1992).
 - [31] O. Gunnarsson, and R.O. Jones, *Phys. Scr.* **21**, 394 (1980).
 - [32] I.I. Mazin, and D.J. Singh, *Phys. Rev. B* **57**, 6879 (1998).
 - [33] P.P. Rushton, D.J. Tozer, and S.J. Clark, *Phys. Rev. B* **65**, 193106 (2002).
 - [34] Z. Wu, R.E. Cohen and D.J. Singh, in AIP conference proceedings volume **677** of *Fundamental Physics of Ferroelectrics* (2003), p. 276, Edited by P.K. Davies and D.J. Singh.
 - [35] Z. Wu, R.E. Cohen, D.J. Singh, R. Gupta, and M. Gupta, *Phys. Rev. B* **69**, 085104 (2004).
 - [36] H. Hellmann, *Einführung in die Quantenchemie* (Deuiecke, Leipzig, 1973), p. 285; R.P. Feynman, *Phys. Rev.* **56**, 340 (1939).
 - [37] N. Troullier, and J.L. Martins, *Phys. Rev. B* **43**, 1993 (1991).
 - [38] P. Gori-Giorgi and J.P. Perdew, *Phys. Rev. B* **66**, 165118 (2002).
 - [39] A.W. Hewat, *J. Phys. C* **6**, 2559 (1973).
 - [40] G.J. Fischer, W.C. Wang, and S. Karato, *Phys. Chem. Minerals*, **20**, 97 (1993). D.A. Berlin-

court, H. Jaffe, Phys. Rev **111**, 143 (1985). L.R. Edwards, R.W. Lynch, J. Phys. Chem. sol., **31**, 573 (1970). E. Wiesendanger, Ferroelectrics **6**, 263 (1974).

TABLE I: Fully relaxed structures of tetragonal PbTiO_3 with the LDA and the GGA. Volumes are in \AA^3 , the numbers in parentheses are the deviations of strain and volume from experiment, and the experimental $c/a = 1.063$.

	volume (Expt.)	c/a	volume (Relaxed)	c/a
LDA	63.28	1.112 (+80%)	60.36 (-4.6%)	1.051 (-20%)
GGA	63.28	1.068 (+7%)	70.58 (+11%)	1.23 (+260%)

TABLE II: Calculated LDA, GGA and WDA lattice constants in \AA for these ferroelectric materials in cubic state, compared with experimental data. Uniform electron gas G was used in the WDA. Numbers in parentheses are deviations from experiment.

material	LDA	GGA	WDA	Expt.
KNbO_3	3.960 (-1.4%)	4.018 (+0.1%)	4.011 (-0.1%)	4.016
KTaO_3	3.931 (-1.3%)	4.032 (+1.2%)	3.972 (-0.3%)	3.983
SrTiO_3	3.858 (-1.2%)	3.935 (+0.8%)	3.917 (+0.3%)	3.905
BaTiO_3	3.951 (-1.4%)	4.023 (+0.6%)	4.009 (+0.2%)	4.000
PbTiO_3	3.894 (-1.9%)	3.971 (+0.1%)	3.941 (-0.7%)	3.969

TABLE III: Optimized internal coordinates of tetragonal PbTiO_3 at the experimental volume ($V = 63.28 \text{\AA}^3$) and strain ($c/a = 1.063$). u_z are given in terms of the lattice constant c . Uniform electron gas G was used in the WDA.

	LDA	GGA	WDA	Expt.
$u_z(\text{Pb})$	0.000	0.000	0.000	0.000
$u_z(\text{Ti})$	0.539	0.532	0.539	0.538
$u_z(\text{O}_{1,2})$	0.615	0.611	0.614	0.612
$u_z(\text{O}_3)$	0.111	0.105	0.110	0.117

TABLE IV: Optimized internal coordinates of rhombohedral BaTiO₃ for the experimental volume ($V = 64.00 \text{ \AA}^3$). u_z are given in terms of the lattice constant. Uniform electron gas G was used in the WDA.

	LDA	GGA	WDA	Expt.
$u_z(\text{Ba})$	0.000	0.000	0.000	0.000
$u_z(\text{Ti})$	0.488	0.488	0.489	0.489
$u_z(\text{O}_1, \text{O}_2)$	0.511	0.510	0.509	0.511
$u_z(\text{O}_3)$	0.020	0.018	0.017	0.018

TABLE V: Optimized internal coordinates of rhombohedral KNbO₃ for the experimental volume ($V = 64.77 \text{ \AA}^3$). u_z are given in terms of the lattice constant. Uniform electron gas G was used in the WDA.

	LDA	GGA	WDA	Expt.
$u_z(\text{K})$	0.507	0.509	0.508	0.5131
$u_z(\text{Nb})$	0.000	0.000	0.000	0.0000
$u_z(\text{O}_1, \text{O}_2)$	0.019	0.024	0.017	0.0313
$u_z(\text{O}_3)$	0.527	0.522	0.520	0.5313

TABLE VI: Volumes (\AA^3) and bulk modulus (GPa) of fully optimized tetragonal PbTiO₃, rhombohedral BaTiO₃ and KNbO₃. Uniform electron gas G was used in WDA. Numbers in parentheses are deviations from experiment. Experimental data are from Refs. [40].

		LDA	GGA	WDA	Expt.
PbTiO ₃	V	60.36 (-4.6%)	70.58 (+11%)	68.46 (+8.2%)	63.28
	B	83	40	42	204
BaTiO ₃	V	61.59 (-3.8%)	67.47 (+5.4%)	66.82 (+4.4%)	64.00
	B	148	94	99	196, 156, 139
KNbO ₃	V	61.96 (-4.3%)	66.63 (+2.9%)	66.04 (+2.0%)	64.77
	B	163	98	114	138

TABLE VII: Calculated WDA (with four types of G denoted in subsection E) lattice constants in \AA for these ferroelectric materials in cubic state. Numbers in parentheses are deviations from experiment.

material	WDA (a)	WDA (b)	WDA (c)	WDA (d)
KNbO ₃	4.011 (-0.1%)	4.018 (+0.0%)	4.006 (-0.2%)	4.001 (-0.4%)
KTaO ₃	3.972 (-0.3%)	3.979 (-0.1%)	3.969 (-0.3%)	3.964 (-0.5%)
SrTiO ₃	3.917 (+0.3%)	3.924 (+0.5%)	3.911 (+0.2%)	3.908 (+0.1%)
BaTiO ₃	4.009 (+0.2%)	4.015 (+0.4%)	4.011 (+0.3%)	4.004 (+0.1%)
PbTiO ₃	3.941 (-0.7%)	3.948 (-0.5%)	3.938 (-0.8%)	3.932 (-0.9%)

TABLE VIII: Volumes of fully optimized tetragonal PbTiO₃, rhombohedral BaTiO₃ and KNbO₃ in \AA^3 using the WDA with two types of G . Numbers in parentheses are deviations from experiment.

	WDA (a)	WDA (d)
PbTiO ₃	68.46 (+8.2%)	63.79 (+0.8%)
BaTiO ₃	66.82 (+4.4%)	65.55 (+2.4%)
KNbO ₃	66.04 (+2.0%)	65.60 (+1.3%)

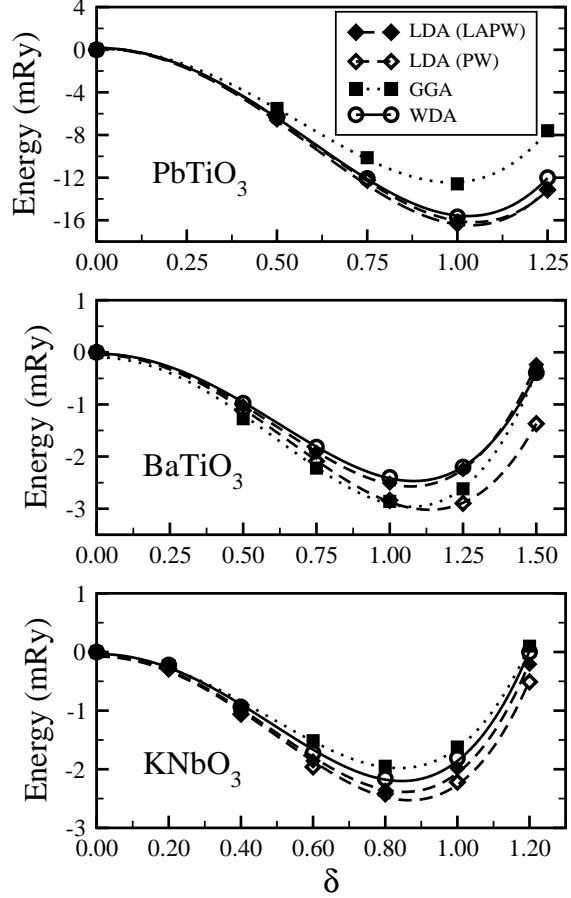


FIG. 1: Total energy as a function of soft-mode displacement in tetragonal PbTiO_3 ($c/a = 1.063$), rhombohedral BaTiO_3 and KNbO_3 with the LDA, GGA, and WDA (uniform electron gas G). Here δ is the displacement relative to experiment.

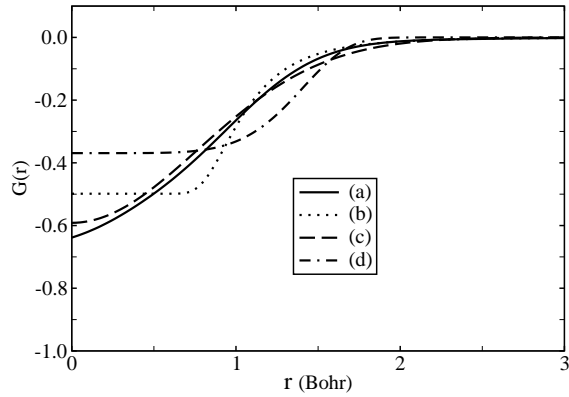


FIG. 2: Four types of function $G(r, n)$ with $r_s = 1.0$ ($n = 0.2387$). (a), (b), (c) and (d) correspond to the types defined in the last subsection of section III.

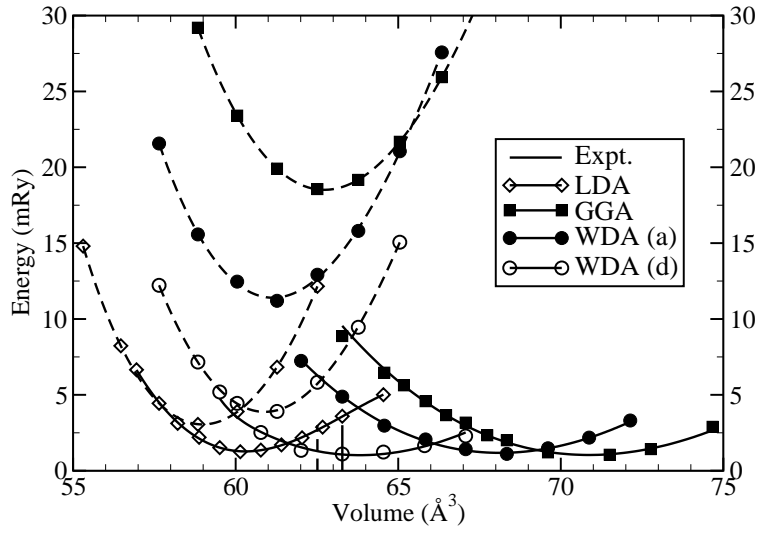


FIG. 3: Energy as a function of volume for the cubic and the relaxed tetragonal PbTiO_3 , with the LDA, GGA, and WDA (two types of G). Dashed lines are cubic structures, and solid lines are tetragonal structures.